Arctic Troposphere Warming Driven by External Radiative Forcing and Modulated by the Pacific and Atlantic

Lingling Suo, Yongqi Gao, Guillaume Gastineau, Yu-chiao Liang, Rohit Ghosh, Tian Tian, Ying Zhang, Young-Oh Kwon, Daniela Matei, Odd Helge Otterå, et al.

JGR Atmospheres

RESEARCH ARTICLE
10.1029/2022JD036679

Arctic Troposphere Warming Driven by External Radiative Forcing and Modulated by the Pacific and Atlantic

Lingling Suo[1], Yongqi Gao[1,2], Guillaume Gastineau[3], Yu-Chiao Liang[4,5,6], Rohit Ghosh[7,8], Tian Tian[9], Ying Zhang[2], Young-Oh Kwon[6], Daniela Matei[8], Odd Helge Otterå[10], and Shuting Yang[9]

[1]Nansen Environmental and Remote Sensing Center and Bjerknes Center for Climate Research, Bergen, Norway, [2]Nansen-Zhu International Research Center, Institute of Atmospheric Physics, Chinese Academy of Sciences, Beijing, China, [3]UMR LOCEAN, CNRS/IRD/MNHN, Sorbonne Université, Paris, France, [4]Department of Atmospheric Sciences, National Taiwan University, Taipei, Taiwan, [5]Lamont-Doherty Earth Observatory, Columbia University, Palisades, NY, USA, [6]Woods Hole Oceanographic Institution, Woods Hole, MA, USA, [7]Department of Meteorology, University of Reading, Reading, UK, [8]Max Planck Institute for Meteorology, Hamburg, Germany, [9]Danish Meteorological Institute, Copenhagen, Denmark, [10]NORCE, Norwegian Research Centre AS, Bjerknes Centre for Climate Research, Bergen, Norway

Abstract During the past decades, the Arctic has experienced significant tropospheric warming, with varying decadal warming rates. However, the relative contributions from potential drivers and modulators of the warming are yet to be further quantified. Here, we utilize a unique set of multi-model large-ensemble atmospheric simulations to isolate the respective contributions from the combined external radiative forcing (ERF-AL), interdecadal Pacific variability (IPV), Atlantic multidecadal variability (AMV), and Arctic sea-ice concentration changes (ASIC) to the warming during 1979–2013. In this study, the ERF-AL impacts are the ERF impacts directly on the atmosphere and land surface, excluding the indirect effects through SST and SIC feedback. The ERF-AL is the primary driver of the April–September tropospheric warming during 1979–2013, and its warming effects vary at decadal time scales. The IPV and AMV intensify the warming during their transitioning periods to positive phases and dampen the warming during their transitioning periods to negative phases. The IPV impacts are prominent in winter and spring and are stronger than AMV impacts on 1979–2013 temperature trends. The warming impacts of ASIC are generally restricted to below 700 hPa and are strongest in autumn and winter. The combined effects of these factors reproduce the observed accelerated and step-down Arctic warming in different decades, but the intensities of the reproduced decadal variations are generally weaker than in the observed.

Plain Language Summary The Arctic tropospheric warming has significant local and remote impacts on the climate and environment. The warming rates vary on the decadal scale. To determine what contributed to the 1979–2013 warming and what drove the variated decadal warming rates, we analyze it with climate models. We find that the combined effects of radiative factors, including solar, greenhouse gases, and aerosols, are the primary driver of the warming except for the winter. The warming rates driven by the radiative factors vary decade by decade. The interdecadal Pacific variability/Atlantic multidecadal variability cools down/warms the Arctic troposphere in this period, while the Pacific impacts are stronger than the Atlantic impacts.

Key Points:

- The external radiative forcing is the primary driver of the 1979–2013 warming for April–September, with varying decadal warming rates
- The interdecadal Pacific and Atlantic multidecadal variability intensify/dampen the warming when transitioning to positive/negative phase
- The combined effects of these factors reproduce the observed varied pace of decadal Arctic troposphere warming during 1979–2013

Supporting Information:

Supporting Information may be found in the online version of this article.

Correspondence to:

L. Suo,
lingling.suo@nersc.no

Citation:

Suo, L., Gao, Y., Gastineau, G., Liang, Y.-C., Ghosh, R., Tian, T., et al. (2022). Arctic troposphere warming driven by external radiative forcing and modulated by the Pacific and Atlantic. *Journal of Geophysical Research: Atmospheres*, *127*, e2022JD036679. https://doi.org/10.1029/2022JD036679

Received 20 MAY 2022
Accepted 29 NOV 2022

1. Introduction

The Arctic is experiencing extensive warming from the surface to the high troposphere, with the surface warming close to four times that of the global average over the last few decades (Cohen et al., 2014; Druckenmiller et al., 2021). The mechanisms of tropospheric warming have not been discussed as widely as surface warming. Still, there is a growing recognition of the importance of the Arctic tropospheric warming in driving mid-latitude weather events. For example, the vertical structure of the Arctic warming is key for a realistic simulated warm Arctic—cold Eurasia pattern: when with imposed tropospheric warming, the Eurasian surface winter cooling is better simulated than with the imposed surface and near-surface warming (He et al., 2020; Labe et al., 2020). Arctic warming can also weaken and shift the Northern Hemisphere jet equatorward and alter the Pacific and Atlantic storm tracks, potentially impacting summer hot-dry extremes (Barnes & Screen, 2015; Coumou et al., 2018).

Table 1
List of Experiments, the Participated Climate Models and the Respective Size of the Ensembles Performed by Each Model, and Total Ensemble Sizes of Individual Experiments

	ALL	ERF2000	ASICClim	NoIPV	NoAMV
CAM6-Nor (Seland et al., 2020)	30	30	30	20	20
EC-Earth3 (Döscher et al., 2021)	20	–	20	20	20
ECHAM6.3 (Stevens et al., 2013)	10	–	10	10	10
IAP4 (Sun et al., 2012)	15	–	15	15	15
IPSL-CM6 (Hourdin et al., 2020)	30	–	30	20	20
CESM2-WACCM6 (Gettelman et al., 2019)	30	–	30	30	30
Total of ensembles	135	30	135	115	115

Assessing the respective contributions of different factors to the Arctic tropospheric warming is essential to better understand the climate changes in the past and to improve future climate projections in both the Arctic and the mid-latitudes. The Arctic sea ice melting alone results in simulated warming restricted to the lower troposphere (Screen & Simmonds, 2010a, 2010b; Zhang et al., 2021). Several other factors have been proposed to explain tropospheric warming. For instance, the sea surface temperature (SST) evolution outside the Arctic and the related atmospheric and oceanic northward meridional heat and moisture transport might significantly contribute (Graversen et al., 2008; Hahn et al., 2021; Henderson et al., 2021; Perlwitz et al., 2015; Screen et al., 2012). A modeling study suggests that the combined natural and anthropogenic radiative forcing partly contributed (<50%) to the summer warming in recent decades (Screen et al., 2012).

Another outstanding question concerns the varying pace of Arctic warming, which could be related to intrinsic multidecadal fluctuations in the climate system (Chylek et al., 2009). Two main modes of SST variability at the decadal to multidecadal time scale might potentially impact the Arctic. One is the Atlantic multidecadal variability (AMV) (Chylek et al., 2009, 2014; Li et al., 2018), and another is the interdecadal Pacific variability (IPV) (Screen & Deser, 2019; Svendsen et al., 2018; Tokinaga et al., 2017). Studies have suggested that the transition of the AMV and the IPV into a positive phase in the early 20th century may have contributed to the Arctic surface warming during that time (Svendsen et al., 2018; Tokinaga et al., 2017). Model simulations have also highlighted the importance of the IPV for driving the Arctic sea ice loss (Screen & Deser, 2019). Whether the evolutions of AMV and IPV have modulated the pace of ongoing Arctic troposphere warming independently of sea ice changes, therefore, needs to be addressed further.

This study tries to single out the primary drivers and the potential modulators of Arctic tropospheric warming. Here, we use a set of multi-model large-ensemble sensitivity experiments to isolate the roles of the external radiative forcing on the atmosphere and land surface (ERF-AL), the internally driven IPV and AMV, and the Arctic sea-ice changes (ASIC) in the Arctic troposphere warming. We will focus on the 1979–2013 period when reliable observations with satellite calibration data are available, and low-frequency variability (IPV and AMV) is well defined.

2. Materials and Methods

Due to the shortage of observations in the Arctic (refers to north of 67°N in this study), the ERA5 reanalysis data set (Hersbach et al., 2020) is used to compare with the climate model output. Comparison with the observational data shows an improved fit regarding the troposphere temperature in ERA5 than the ERA-Interim (Hersbach et al., 2020). Previous studies have also evaluated the performance of the ERA5 data in the Arctic region. ERA5 2 m temperature is highly correlated (0.95) with the 2010–2020 buoy observations north of 70°N, although it presents generally warm biases (Yu et al., 2021). The lower-mid troposphere temperature in ERA5 has the best correlation coefficients (generally above 0.95 in different pressure levels) with a radiosonde observation over the Fram Strait in 2017 late summer among five reanalysis data sets (Graham et al., 2019).

Five sets of state-of-the-art Atmosphere General Circulation Model experiments starting from 1 January 1979, as listed in Table 1, are analyzed: (a) ALL: the historical hindcast experiment with the daily SST and sea ice concentration (SIC) from the HadISST 2.2.0.0 (Titchner & Rayner, 2014) and with the Coupled Model Intercomparison

Project Phase 6 (CMIP6) external forcing (Eyring et al., 2016); (b) ERF2000: same as ALL but with the external natural and anthropogenic radiative forcing as 1995–2005 mean which is a verified build-in present-day climate external forcing set in CAM6 and is closer to the radiative forcing level in the concerned period than the pre-industrial climatology; (c) ASICClim: same as ALL but with the daily Arctic SIC and Arctic SST as 1979–2014 mean; (d) and (e): NoIPV and NoAMV: same as ALL but with the IPV signals in the Pacific and AMV signals in the north Atlantic removed from the daily SST. Arctic sea ice thickness fields are constant in our simulation. The IPV and AMV signals adopted in our simulations are from the decadal climate prediction project (Boer et al., 2016) panel of CMIP6 (See the Data availability part for the DOI). The IPV and AMV are the estimated internal component of the observed decadal variability by using the signal-to-noise maximizing EOF (Ting et al., 2009) to remove the effect of the external forcing. The IPV and AMV data are till 2013. More technical details about how to obtain IPV and AMV can be found in: https://www.wcrp-climate.org/wgsip/documents/Tech-Note-1.pdf.

The impacts of factors are obtained as the following. Both the ALL and ERF2000 utilize the historical observational SST and SIC as the boundary conditions, in which their feedbacks to ERF are included. By subtracting the results of ERF2000 (30 ensembles mean) from ALL (also 30 ensembles mean accordingly performed by CAM6-Nor), the ERF impacts on the atmosphere and land surface, excluding the indirect effects through SST and SIC feedbacks, hereafter ERF-AL impacts, are isolated. The ASIC, IPV, and AMV impacts are obtained by subtracting the all ensemble means of ASICClim, NoIPV, and NoAMV from that of ALL. The IPV and AMV impacts are the impacts of the internally driven decadal variability of Pacific and north Atlantic SST. The difference of the experiments by ALL minus the others estimates the influence of the respective factor, accounting for interactions with the other un-fixed components in the climate system. Each ensemble, independently of the model, has the same weight in computing the ensemble means. The multi-model ensemble mean is calculated by averaging all ensemble members with equal weight.

Trends in the ERA5 and each member of the simulations are computed by a least-squares fit of the linear regression. A two-tailed *t*-test verifies the statistical significance of the trend with a null hypothesis that the trend is zero. The trend is statistically significant at the 5% level when the corresponding probability value is less than 0.05. The ensemble mean of the trends in each experiment is computed. The independent two-sample *t*-test is used to examine whether the means from the different groups are statistically different (i.e., the impacts are statistically significant) with a stipulated significance level at 0.05 (Santer et al., 2000). The difference significance test is to verify if a factor or factors could drive a significant change between the two mean statuses. A statistically significant difference between the trends could also happen in the region where a trend is insignificant in the individual experiment.

3. Results

3.1. Attribution of the Arctic Temperature Trend During the Period 1979–2013

The Arctic troposphere temperature trends during 1979–2013 in ERA5 (Figure 1a) are similar to previous studies based on various reanalysis data sets (Liang et al., 2021; Screen et al., 2012): the warming is from the surface to the upper troposphere during the whole year, with the most significant warming occurring below 850 hPa during autumn and winter. ALL generally reproduce the seasonality and vertical structure of the observed patterns with about 0.2°C/0.1°C higher warming trend in the mid-troposphere during summer and autumn/winter (Figure 1b). ALL underestimates the warming below 850 hPa in April, and such underestimation was also presented by previous studies (Hahn et al., 2021; Screen et al., 2012). The winter warming and spring cooling above 300 hPa in ERA5 are generally not statistically significant and not found in ALL. Note the trends in ERA5 may be influenced by the internal atmospheric variability, while ALL largely suppressed such influence by taking the ensemble mean. There are individual members in ALL that reproduce the similar February 200 hPa warming, April 200 hPa cooling, and April near-surface warming as shown in ERA5 (Figure S1 in Supporting Information S1).

The simulated Arctic warming is strongly controlled by the ERF-AL throughout the troposphere from April to September (Figure 2a). The ERF-AL driven warming is up to 0.5°C/decade in the lower-mid troposphere during the summer season. In February, March, and October, the warming caused by ERF-AL is about 0.1–0.2°C/decade from the near-surface to the lower troposphere and not statistically significant in the mid-troposphere. There is no statistically significant contribution of ERF-AL during November–January when little solar irradiations arrive at

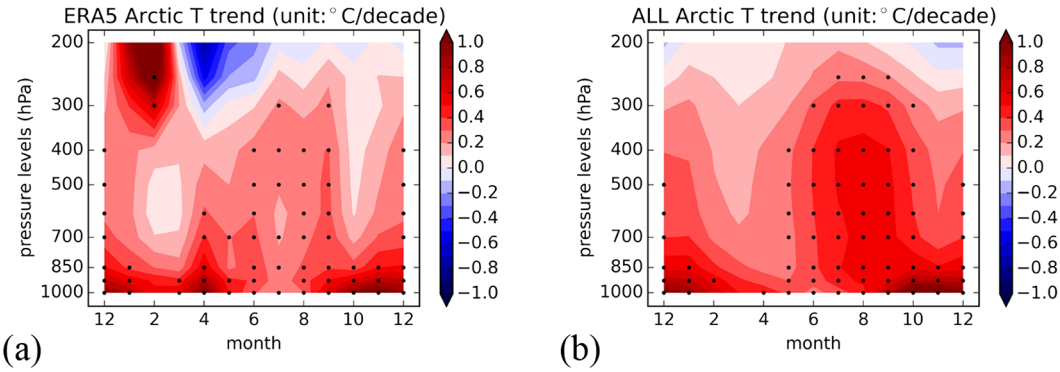

Figure 1. Monthly-vertical distribution of the area-weighted Arctic (north of 67°N) temperature linear trends during 1979–2013 in (a) ERA5 and (b) ALL. Dots mark where the linear trends are statistically significant. The color interval is 0.1.

the North Pole. The seasonality of the radiative forcing could be a reason for ERA-AL impacts seasonality. The ERF-AL impacts include the feedbacks from the albedo and evapotranspiration changes in the land surfaces. That also contributes to the seasonality of the ERF-AL driven warming: the lower albedo, higher evapotranspiration, and more latent heat flux into the atmosphere appear in spring-summer seasons, accompanying with warmer landmasses (Flanner et al., 2011). The ERF-AL impacts on SAT over land regions do show seasonality, with peak warming in the spring-summer seasons (Figure S2 in Supporting Information S1).

The ERF-AL explains as much as 50%–80% of Arctic tropospheric warming and should be considered the primary driver during April–September (Figure 2b). The ERF-AL impact explains about 30%–40% of the lower-troposphere Arctic warming in February, March, and October. The ERF-AL contributes little to the winter Arctic warming, while the indirect impacts on the ASIC and SST are excluded. But radiative forcing could indirectly increase winter warming by increasing ice melt and seasonal ocean heat storage (Bintanja & Krikken, 2016). Interestingly, the ERF-AL impact presented in this study is more extensive and intensive than that identified by Screen et al. (2012) using a similar methodology, where the impact of ERF on Arctic warming was weak in July–August (Screen et al., 2012). This implies the uncertainty of the simulated ERF-AL effects, with a potential influence of the prescribed external forcing or the inter-model differences in the surface albedo and cloud feedbacks (Block et al., 2020; Zhang et al., 2018). The selection of the period could also be a possible reason for the difference: 1979–2013 is selected in this study, while 1979–2008 is analyzed in Screen et al. (2012).

The ASIC has been recognized as the main driver of the surface and near-surface warming in autumn and winter as the ocean heat release is amplified when sea-ice retreats and becomes thinner (Dai et al., 2019; Screen & Simmonds, 2010a; Zhang et al., 2021). The ASIC impact simulated here agrees with the assertion from the previous works (Labe et al., 2020; Screen et al., 2012; Screen & Simmonds, 2010a). The warming caused by sea ice decline is confined to the near-surface and the lower troposphere, with the most significant warming (around 0.9°C/decade) located at the near-surface during October–November (Figure 2c), which explains up to 80% of the warming simulated by ALL (Figure 2d). ASIC causes statistically significant warming up to 300 hPa in February and summer, but the amplitude remains weak (about 0.1°C/decade) compared to the observed trends. However, the Arctic sea ice thickness fields are constant in our simulation. The inclusion of the thinning sea ice thickness in the model would increase the heat fluxes (Landrum & Holland, 2022) and intensify the simulated Arctic warming in the cold season (Labe et al., 2018; Lang et al., 2017; Sun et al., 2018).

The IPV shows a considerable cooling impact on the Arctic temperature during October–May throughout the troposphere (Figure 2e). The most significant cooling caused by IPV is in March–April from the lower to the upper troposphere and November–December in the lower-mid troposphere, with about −0.2°C/decade. The cooling intensity is about 40% of the simulated November–December warming and exceeds 60% of the simulated March–April warming in ALL (Figure 2f). Such tropospheric cooling is consistent with the teleconnections from the IPV shifts from a warm phase between 1980 and 1998 to a cold phase after 2005 (Figure 3a). Indeed, a declining IPV is well known to lead to a trend toward a weakening Aleutian low (an anomalous high over the northern North Pacific), with an anomalous low over northern North America and the Arctic, in the extended winter season (Mantua & Hare, 2002; Trenberth & Hurrell, 1994; Zhang et al., 1997). Such a pattern can decrease the northward

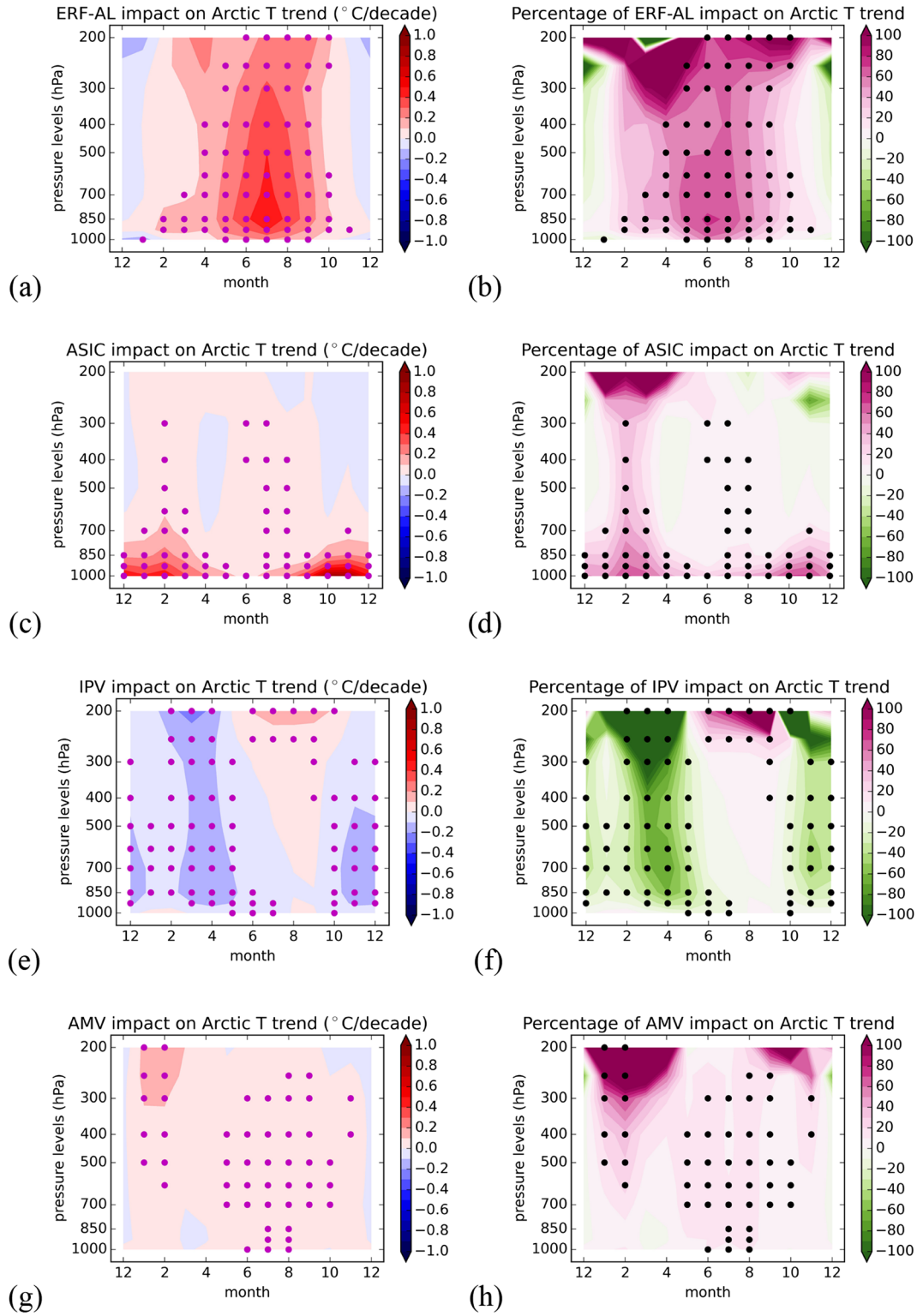

Figure 2. Monthly-vertical distribution of the simulated impacts of (a) ERF-AL, (c) ASIC, (e) IPV, and (g) AMV to the area-weighted Arctic (north of 67°N) temperature linear trends during 1979–2013. And the ratios of (b) ERF-AL, (d) ASIC, (f) IPV, and (h) AMV impacts with respect to the Arctic temperature trend simulated in ALL. The ERF-AL/other results are based on the simulations from CAM6-Nor only/all models. The dots mark where the impacts are statistically significant at the 5% level. The color interval is 0.1 for the impacts and 10% for the ratios.

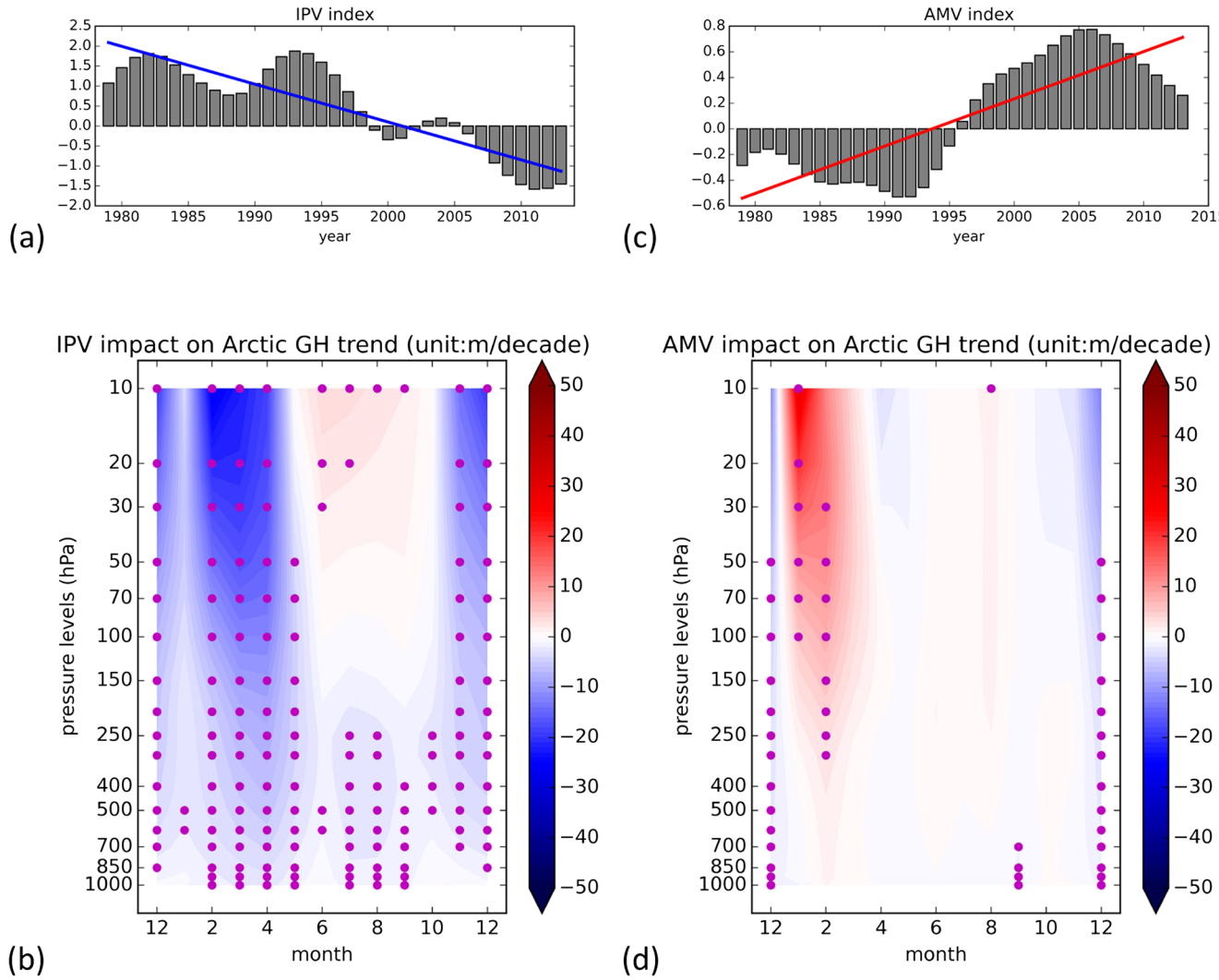

Figure 3. (a) IPV and (c) AMV index (bar) from CMIP6 input4MIP DCPP and the linear trends (line) during 1979–2013. (b) and (d) show the monthly-pressure level distribution of IPV and AMV impact on the Arctic Geopotential height (GH) trend. The dots indicate where the impacts are statistically significant at the 5% level.

atmospheric heat transport into the troposphere Arctic and reduce the November–December upward propagating waves into the stratosphere, resulting in a strengthened and colder stratospheric winter polar vortex (Svendsen et al., 2018; Woo et al., 2015). Subsequently, stratospheric circulation changes can propagate downward to affect the troposphere after up to 2 months into spring (Baldwin & Dunkerton, 2001; Baldwin et al., 2003; Polvani & Waugh, 2004). The monthly-pressure level distribution of the IPV impacts on the Arctic geopotential height trend explicitly supports the mentioned troposphere-stratosphere-troposphere process (Figure 3b). The spatial distributions of the IPV impacts are shown in Figure S3 in Supporting Information S1. In our simulation, the anomalous low centered over northern North America in November–December is strengthened and tilted to the central Arctic in March–April, indicating the strengthened stratospheric polar vortex descending into the troposphere in spring superimposed on the implication of the weakened Aleutian low.

The AMV shows a weak warming impact on the troposphere Arctic during 1979–2013 generally throughout the year, which is statistically significant during the extended summer season (May–October) and January–February (Figure 2g). During January–February, the warming is most intensive (about 0.2°C/decade) in the upper troposphere. The warming driven by AMV is about equivalently 20% of the May–October warming and more than 50% of the January–February upper troposphere warming in ALL (Figure 2h). Such warming accompanies an increasing AMV index during this period (Figure 3c). Although previous studies have suggested that the warm (positive) AMV phase intensified Arctic surface warming (Li et al., 2018; Tokinaga et al., 2017), exactly how the

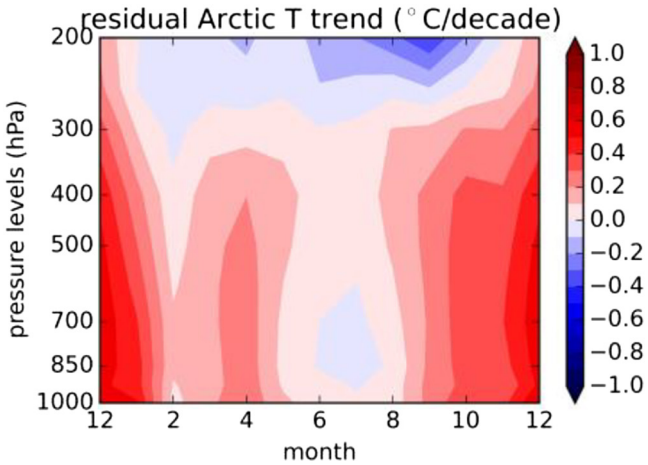

Figure 4. Residual Arctic Temperature trends by Figure 1b minus the sum of Figures 2a, 2c, 2e, and 2g. The color interval is 0.1.

AMV modulates Arctic tropospheric warming is not clear. Our simulations indicate that AMV drives a weakening of the polar vortex and associated warming over the Arctic region in January–February (Figure 3d), with the anomalies centered over the Atlantic side (Figures S4a–S4d in Supporting Information S1). Such a weakening of the polar vortex is consistent with previous work (Omrani et al., 2014). In our simulations, the AMV changes also produce weak atmosphere responses in summer, with two small geopotential height positive anomalies located over the northern North Atlantic and northeast Eurasia and widespread warming over the Northern Hemisphere at 500 hPa (Figures S4e and S4f in Supporting Information S1). The detailed processes involved in AMV driving these anomalies still need to be further explored in future studies. However, since the AMV change during the 1979–2013 period is relatively modest compared to other past observed changes within the instrumental period, the atmospheric changes induced by AMV only have a minor impact on the Arctic tropospheric warming in these climate model experiments.

Residual Arctic temperature trends are obtained by the Arctic temperature trends in ALL minus the sum of the ERF-AL, ASIC, IPV, and AMV impacts, which present significant warming from October to January throughout the troposphere and April warming with relative weaker intensity in the low-mid troposphere (Figure 4). This indicates that some other reasons besides the factors concerned in this study caused the Arctic winter troposphere warming. The possible candidates could be the SSTs outside of the Pacific and Atlantic or the SST variabilities not explained by IPV and AMV in the Pacific and Atlantic. And also, the residual trends are based on the assumption that the effects of individual factors are linearly summable. However, the total effects of all the factors might be different from the simple sum-up because of the interactions in the complex climate system. Thus, the total effects of the factors and the unexplained part of the warming need further investigation.

In summary, during 1979–2013, ERF-AL contributes to significant warming in the Arctic throughout the troposphere except for the winter. IPV contributes a substantial cooling in winter and spring, while AMV contributes weak warming. The contribution of ASIC is confined to the near-surface and lower troposphere and can explain most of the warming there. Since the ERF-AL impacts are isolated from CAM6-Nor output while the other impacts are analyzed based on six models output, we also present the ASIC, IPV, and AMV impacts on Arctic temperature trends obtained solely from the CAM6-Nor ensembles for comparison (Figure S5 in Supporting Information S1). They are very close to those demonstrated in Figure 2.

3.2. Evolution of the Decadal Trend of the Arctic Temperature

As presented in the previous section, the phase transition of AMV and/or IPV modulated the multidecadal Arctic temperature variability during 1979–2013. There are several fluctuations in the IPV/AMV index during this period. For example, the AMV index moves downward/upward/downward in the 1980s/1990s/after 2005 (Figure 3c). On the other hand, the melting of the Arctic sea ice has increased steadily, even accelerating since 2000 (Druckenmiller et al., 2021). Therefore, a natural question is: what are the respective contributions of ERF-AL, ASIC, IPV, and AMV to the evolution of the decadal Arctic annual-mean temperature trend?

Figure 5 shows the evolution of the impacts of ERF-AL, ASIC, IPV, and AMV on the 10-year running trend of Arctic annual-mean temperature. The ERF-AL warms the Arctic during the whole period with two subperiods of slower warming/weak cooling: the first period from 1984–1993 to 1988–1997, and the second period around 1999–2008 (Figure 5a). The warming rates driven by ERF-AL are highest during the decades from 1990–1999 to 1995–2004. Figure 5a presents the combined impacts of natural and anthropogenic ERF. According to our experimental design, it is not feasible to isolate the effects of an individual forcing. However, we can discuss the possible causes of such decadal variations based on observational records and previous studies. The increasing greenhouse gases have been suggested as the primary cause of Arctic warming as part of global warming (Chylek et al., 2014; Gillett et al., 2008; Liang et al., 2022). The injection of sulfur aerosol into the stratosphere by the eruption of Mount Pinatubo in 1991, the most massive volcanic eruption in the second half of the 20th century, resulted in a clear negative radiative forcing (Chylek et al., 2014). The associated volcanic aerosol loading into

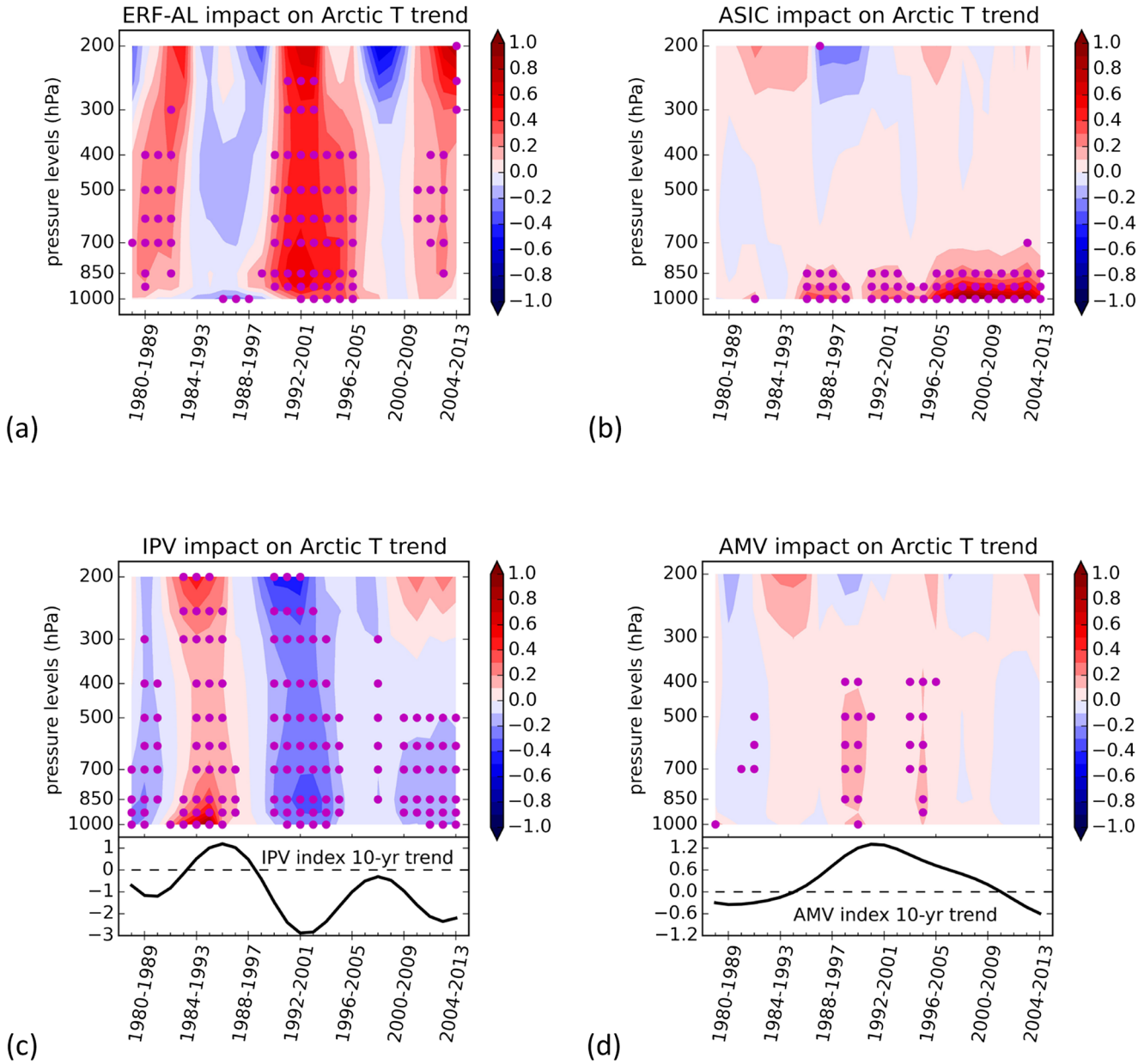

Figure 5. Impacts of (a) ERF-AL, (b) ASIC, (c) IPV, and (d) AMVon the 10-year running trends of annual-mean Arctic temperature (colored, unit: ℃/decade), and the 10-year running trend of the IPV/AMV index (line) shown below the IPV/AMV impacts. The years marked in the plot indicate the period for the calculation. The dots mark where the impacts are statistically significant.

the stratosphere cooled the world in 1992 and the subsequent two years (Parker et al., 1996). And the cooling also reached and covered the Arctic (Yang & Schlesinger, 2002), thus interrupting the warming trend around 1985–1994. The Arctic anthropogenic tropospheric aerosol (sulfate and black carbon) loading peaked in the late 1980s and declined sharply in the 1990s (Breider et al., 2017; Hirdman et al., 2010). Thus, the negative radiative forcing of anthropogenic sulfate tropospheric aerosol over the Arctic is most significant in the 1980s and gets weaker in the 1990s, which intensifies the decadal warming trends starting from the early 1990s. The net cooling by decreasing black carbon is minor compared with the sulfate aerosol effects (Ren et al., 2020). During 1999–2008, the warming caused by rising greenhouse gas concentrations was counteracted by the mixed effects of declining solar irradiation to its minimum around 2009 as part of the 11-year cycles (Matthes et al., 2017) and the rapid growth of anthropogenic aerosols (Kaufmann et al., 2011). The IPV is in its negative phase after 2005

(Figure 3a), which could potentially amplify the effects of solar irradiance proposed by a recent modeling study (Guttu et al., 2021).

The warming contributed by ASIC is confined below 700 hPa, intensifying since 1985 (Figure 5b), coinciding with the acceleration of sea-ice melting (Figure S6 in Supporting Information S1). The warming rate near-surface increases from around 0.3°C/decade during 1986–1995 to around 1°C/decade after 1996, which corresponds well with the intensified sea-ice retreat.

The effects of IPV and AMV on the decadal temperature trend coincide with the interdecadal shifts of their respective indices (Figures 5c and 5d). When the associated 10-year trend of the IPV (or AMV) index is positive (i.e., index rising)/negative (i.e., index declining), the corresponding warming/cooling impacts appear. The stronger the IPV and AMV changes are, the stronger the Arctic temperature responses. The cooling contributed by IPV is strongest during the decades starting in 1990–1995, at −0.4°C/decade in the lower and higher troposphere. The warming contributed by AMV is strongest in the 1990s, about 0.2°C/decade. The modulation by IPV is generally larger than that by AMV.

Since the effects of the ERF-AL and IPV are mainly in the extended summer and winter season, respectively, the impacts of ERF-AL, ASIC, IPV, and AMV on the decadal trends of Arctic temperature in boreal summer and winter half-year are presented for comparison (Figure 6). The summer half-year refers to April–September, and the winter half-year refers to the rest 6 months. In general, the ERF-AL warming impacts on the decadal trends are similar to but intensified in the summer half-year than the annual mean. In contrast, its cooling impacts in the decades from 1984–1993 to 1988–1997 are more significant in the winter half-year, with the volcanic aerosols' effects emerging: Besides the cooling by scattering back of the solar irradiation in the polar summer season, the volcanic aerosols absorb solar near-infrared and terrestrial infrared radiations but more in the low latitudes than in the Arctic during the winter season, which drives an intensified meridional temperature gradient and a strengthened colder polar vortex (Robock, 2000; Stenchikov et al., 2002). The impacts on the decadal trends from AMV are similar to their respective annual-mean pattern but intensify in the summer half-year and are less significant in the winter half-year, while the IPV and ASIC impacts intensify in the winter-half year and are weaker in the summer half-year.

The contributions of the individual factors to the Arctic tropospheric warming vary in different decades. Can they drive the observed decadal variations of the Arctic temperature warming rates? We do not expect that these factors can give the full attribution. Indeed, the estimated variance of the IPV and AMV time-evolving pattern in 1979–2013 only represents 15.6% of the total SST estimated variance north of 20°N (Text S1 in Supporting Information S1). And apart from the IPV and AMV fluctuations, the SST north of 20°N shows a mean warming trend of 0.18°C/decade that we did not take into consideration (Text S1 in Supporting Information S1). Here, we want to verify if the combined effects of ERF-AL, IPV, AMV, and ASIC, which include the key drivers of the decadal variability in the Northern Hemisphere, are significant enough to drive the key decadal variations of the Arctic warming rates.

To better isolate the fluctuation of the Arctic 10-year temperature trends, the deviations obtained by removing the long-term (1979–2013) trends are shown in Figure 7 for the levels where the long-term trends are statistically significant (up to 300 hPa in ALL, Figure S7 in Supporting Information S1). Figure 7a shows the deviations of the running decadal trends minus 1979–2013 trends in ERA5. And Figure 7b shows the sum of the deviations of the ERF-AL, ASIC, IPV, and AMV impacts on the decadal temperature trends minus the corresponding respective impacts on the 1979–2013 trends. The 10-year trends in ERA5 are greater than the whole period trends from 1989–1998 to 1998–2007 decades (middle period) and below the long-term trends in the decades starting from 1979 to 1988 (early period) and after 1999 (later period; Figure 7a). The middle-period accelerated warming is about two to three times the long-term trend in the lower-mid troposphere. The combined effects of ERF-AL, IPV, AMV, and ASIC reproduce key features of the accelerated warming in the middle period and decelerated warming in the early and later periods, although deviation intensities are about half in the early-middle periods than those in ERA5 (Figure 7b). The similarity between Figures 7a and 7b demonstrates the notion that the factors considered in this study should be the key factors driving the interdecadal variations of Arctic warming.

A potential reason for the weaker deviations in the model simulations could be the exclusion of the externally forced multidecadal SST variations in the Pacific and Atlantic that can intensify the decadal deviations when in phase with the internally driven signals (Meehl et al., 2013; Ting et al., 2009). The SSTs outside of the Pacific and

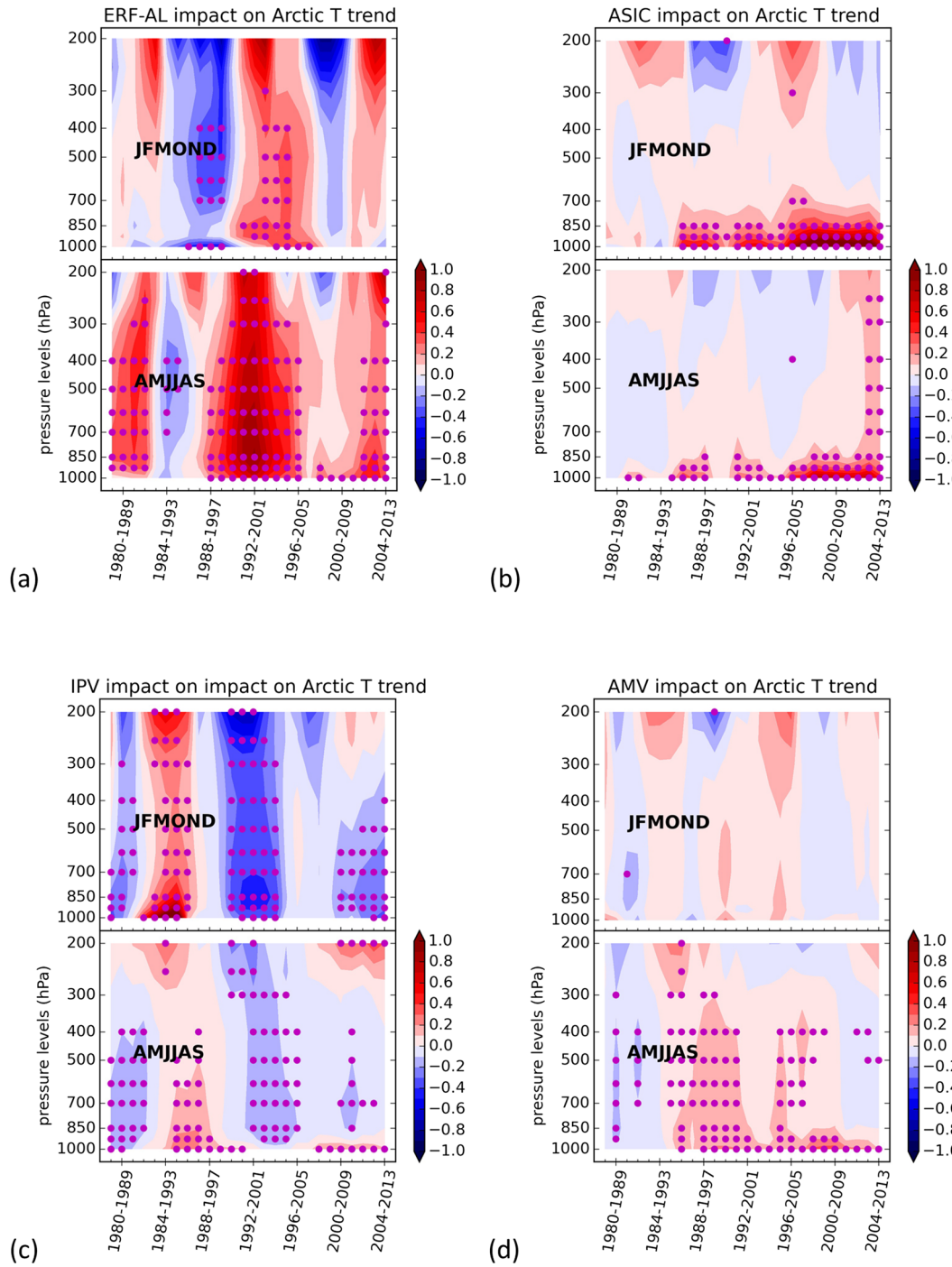

Figure 6. Similar to Figure 5 but for the impacts on the 6-month mean Arctic temperature (colored, unit: ℃/decade). AMJJAS: April-September (the boreal summer half-year); JFMOND: the rest six months (the boreal winter half-year).

Atlantic might also play a role. And if the total effects of all the factors would be stronger than the simple sum-up because of their interactions is also a question to answer.

There are also three sub-periods in ALL with the below/above/below average warming rates (Figure 7c). The deviations in ALL are similar to those in ERA5 except that: (a) the negative deviations are more intense after 2000–2009 and (b) from 1983–1992 to 1988–1997, the deviations are opposite between ERA5 and ALL. The reduced warming around 1984–1993 in ERA5 is not found in Figures 7b and 7c. However, the ERA5 1984–1993

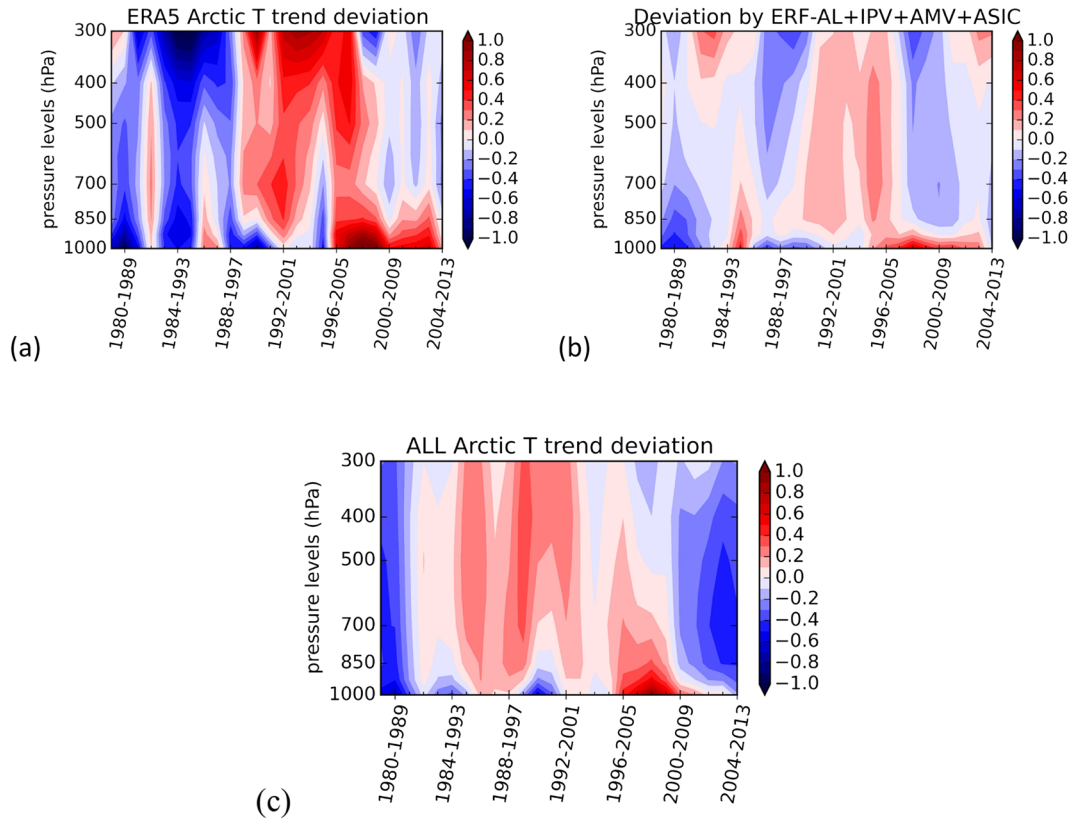

Figure 7. Deviations of the Arctic annual-mean temperature 10-year trends (a) relative to the 1979–2013 trends in ERA5, (b) reconstructed by the sum of the individual deviations of ERF-AL, IPV, AMV, and ASIC decadal impacts relative to their respective impacts on 1979–2013 trends, and (c) relative to the 1979–2013 trends in ALL (unit: ℃/decade). The years marked in the plot indicate the period for the calculation of the 10-year trend.

trend deviation is located at the tail of the distribution of the ALL ensembles (Figure S8 in Supporting Information S1). This indicates that such a difference may result from internal variability in ERA5, while internal variability is largely removed by applying the ensemble mean. The reduced warming around 1988–1997 in ERA5 is well presented by the combined effects of ERF-AL, IPV, AMV, and ASIC, but there is accelerated warming in ALL during the same period, which should be attributed to other factors, possibly SSTs in other regions and other uncovered factors.

4. Conclusions and Discussion

This study has explored the potential causes of Arctic tropospheric warming and the decadal variations of its warming rates. The ERF-AL contributes a large part to the warming from April to September during 1979–2013. The warming rates caused by ERF-AL vary from decade to decade, with different individual forcing (i.e., greenhouse gases, volcanic forcing, tropospheric aerosols, solar, etc.) prevailing in the respective period. The IPV and the AMV are two key modulators of the Arctic temperature changes. The ASIC impact is mostly confined to the lower troposphere.

This study does not take into account the indirect influence through the impact of one factor on other factors. For example, the isolated impacts of ERF-AL or IPV in this study don't include the indirect effects from the ASIC changes driven by ERA-AL or IPV. The mechanisms involved in their interactions and the potential predictive nature of the factors are still largely uncertain. However, the shifts of IPV and AMV between positive and negative phases and the solar cycle continue. Thus, it is expected that there would have possible slowdowns and accelerations of Arctic warming again. Our study has a limitation with a stop at 2013, and after the 2000s warming hiatus, the Arctic warming accelerated again (Ballinger et al., 2021). As shown in Figure S9 in Supporting Information S1, with the decadal trend deviations relative to the 1979–2013 trend extended to 2012–2021, the

accelerated Arctic warming is throughout the troposphere, and the most intensive decadal warming happened in 2008–2017. IPV transposed from the negative phase to the positive after 2015 until 2018 (https://www.ncdc.noaa.gov/teleconnections/pdo/). And the solar forcing kept rising after 2010 and reached its top level of the circle about 2015 (Egorova et al., 2018; Matthes et al., 2017). They both can be the possible accelerators of Arctic warming in this period. However, the effects need to be further verified and confirmed by extending our study to date. Furthermore, AMV has been shown to be predictable to a large degree at a decadal time scale, and IPV is also suggested to be predictable with less predictability than AMV (Keenlyside et al., 2008; Mochizuki et al., 2010). That could supply some potential for predicting future Arctic warming.

Our study has further implications for the mid-latitudes climate change. Recent studies suggest that the strength of the Arctic tropospheric warming is important for isolating the link with winter Eurasian weather (He et al., 2020; Labe et al., 2020). The link of the Arctic tropospheric warming to the mid-latitudes climate change in other seasons also needs to be studied. The roles of different factors in driving the Arctic tropospheric temperature vary period by period and season by season. That implies that the connections between Arctic and mid-latitudes and underlying mechanisms vary between periods and seasons.

Data Availability Statement

ERA5 data is obtained through Copernicus Climate Change Service (C3S) Climate Data Store (CDS) (https://doi.org/10.24381/cds.6860a573) (Hersbach et al., 2019). IPV data is in http://doi.org/10.22033/ESGF/input4MIPs.1119 (Cassou, 2017b). AMV data is in http://doi.org/10.22033/ESGF/input4MIPs.1113 (Cassou, 2017a). HadISST 2.2.0.0 is obtained from https://www.metoffice.gov.uk/hadobs/hadisst2/ (Met Office Hadley Centre, 2016). The core model output used in this study is available through Norwegian research infrastructure services (http://ns9015k.web.sigma2.no/BlueAct/) (Suo et al., 2022).

Acknowledgments
This work is funded by the European Union's Horizon 2020 research and innovation program 727852 Blue-Action Project, JPI Climate-Oceans ROADMAP, the Danish national funded National Centre for Climate Research (NCFK, Nationalt Center for Klimaforskning), National Key R&D Program of China 2017YFE0111800, and NSF OPP-1736738 & OPP-2106190. The CAM6-Nor simulations were performed on resources provided by UNINETT Sigma2—the National Infrastructure for High Performance Computing and Data Storage in Norway (nn2343k, NS9015K).

References

Baldwin, M. P., & Dunkerton, T. J. (2001). Stratospheric harbingers of anomalous weather regimes. *Science*, *294*(5542), 581–584. https://doi.org/10.1126/science.1063315

Baldwin, M. P., Stephenson, D. B., Thompson, D. W., Dunkerton, T. J., Charlton, A. J., & O, N. A. (2003). Stratospheric memory and skill of extended-range weather forecasts. *Science*, *301*(5633), 636–640. https://doi.org/10.1126/science.1087143

Ballinger, T. J., Overland, J. E., Wang, M., Bhatt, U. S., Brettschneider, B., Hanna, E., et al. (2021). Surface air temperature. https://doi.org/10.25923/53xd-9k68

Barnes, E. A., & Screen, J. A. (2015). The impact of Arctic warming on the midlatitude jet-stream: Can it? Has it? Will it? *Wiley Interdisciplinary Reviews: Climate Change*, *6*(3), 277–286. https://doi.org/10.1002/wcc.337

Bintanja, R., & Krikken, F. (2016). Magnitude and pattern of Arctic warming governed by the seasonality of radiative forcing. *Scientific Reports*, *6*(1), 38287. https://doi.org/10.1038/srep38287

Block, K., Schneider, F. A., Mülmenstädt, J., Salzmann, M., & Quaas, J. (2020). Climate models disagree on the sign of total radiative feedback in the Arctic. *Tellus A: Dynamic Meteorology and Oceanography*, *72*(1), 1–14. https://doi.org/10.1080/16000870.2019.1696139

Boer, G. J., Smith, D. M., Cassou, C., Doblas-Reyes, F., Danabasoglu, G., Kirtman, B., et al. (2016). The decadal climate prediction project (DCPP) contribution to CMIP6. *Geoscientific Model Development*, *9*(10), 3751–3777. https://doi.org/10.5194/gmd-9-3751-2016

Breider, T. J., Mickley, L. J., Jacob, D. J., Ge, C., Wang, J., Payer Sulprizio, M., et al. (2017). Multidecadal trends in aerosol radiative forcing over the Arctic: Contribution of changes in anthropogenic aerosol to Arctic warming since 1980. *Journal of Geophysical Research: Atmospheres*, *122*(6), 3573–3594. https://doi.org/10.1002/2016JD025321

Cassou, C. E. (2017a). input4MIPs.CNRM-Cerfacs.SSTsAndSeaIce.DCPP.DCPP-C-amv-1-1 [Dataset]. Earth System Grid Federation. https://doi.org/10.22033/ESGF/input4MIPs.1113

Cassou, C. E. (2017b). input4MIPs.CNRM-Cerfacs.SSTsAndSeaIce.DCPP.DCPP-C-ipv-1-1 [Dataset]. Earth System Grid Federation. https://doi.org/10.22033/ESGF/input4MIPs.1119

Chylek, P., Folland, C. K., Lesins, G., Dubey, M. K., & Wang, M. (2009). Arctic air temperature change amplification and the Atlantic Multidecadal Oscillation. *Geophysical Research Letters*, *36*(14), L14801. https://doi.org/10.1029/2009GL038777

Chylek, P., Hengartner, N., Lesins, G., Klett, J. D., Humlum, O., Wyatt, M., & Dubey, M. K. (2014). Isolating the anthropogenic component of Arctic warming. *Geophysical Research Letters*, *41*(10), 3569–3576. https://doi.org/10.1002/2014GL060184

Cohen, J., Screen, J. A., Furtado, J. C., Barlow, M., Whittleston, D., Coumou, D., et al. (2014). Recent Arctic amplification and extreme mid-latitude weather. *Nature Geoscience*, *7*(9), 627–637. https://doi.org/10.1038/ngeo2234

Coumou, D., Di Capua, G., Vavrus, S., Wang, L., & Wang, S. (2018). The influence of Arctic amplification on mid-latitude summer circulation. *Nature Communications*, *9*(1), 2959. https://doi.org/10.1038/s41467-018-05256-8

Dai, A., Luo, D., Song, M., & Liu, J. (2019). Arctic amplification is caused by sea-ice loss under increasing CO_2. *Nature Communications*, *10*(1), 121. https://doi.org/10.1038/s41467-018-07954-9

Döscher, R., Acosta, M., Alessandri, A., Anthoni, P., Arneth, A., Arsouze, T., et al. (2021). The EC-Earth3 Earth system model for the climate model intercomparison project 6. In *Geoscientific model development discussion, 2021* (pp. 1–90). https://doi.org/10.5194/gmd-2020-446

Druckenmiller, M. L., Moon, T. A., Thoman, R. L., Ballinger, T. J., Berner, L. T., Bernhard, G. H., et al. (2021). The Arctic. *Bulletin of the American Meteorological Society*, *102*(8), S263–S316. https://doi.org/10.1175/BAMS-D-21-0086.1

Egorova, T., Schmutz, W., Rozanov, E., Shapiro, A. I., Usoskin, I., Beer, J., et al. (2018). Revised historical solar irradiance forcing. *A&A*, *615*, A85. https://doi.org/10.1051/0004-6361/201731199

Eyring, V., Bony, S., Meehl, G. A., Senior, C. A., Stevens, B., Stouffer, R. J., & Taylor, K. E. (2016). Overview of the Coupled Model Intercomparison Project Phase 6 (CMIP6) experimental design and organization. *Geoscientific Model Development*, *9*(5), 1937–1958. https://doi.org/10.5194/gmd-9-1937-2016

Flanner, M. G., Shell, K. M., Barlage, M., Perovich, D. K., & Tschudi, M. A. (2011). Radiative forcing and albedo feedback from the Northern Hemisphere cryosphere between 1979 and 2008. *Nature Geoscience*, *4*(3), 151–155. https://doi.org/10.1038/ngeo1062

Gettelman, A., Mills, M. J., Kinnison, D. E., Garcia, R. R., Smith, A. K., Marsh, D. R., et al. (2019). The whole atmosphere community climate model version 6 (WACCM6). *Journal of Geophysical Research: Atmospheres*, *124*(23), 12380–12403. https://doi.org/10.1029/2019JD030943

Gillett, N. P., Stone, D. A., Stott, P. A., Nozawa, T., Karpechko, A. Y., Hegerl, G. C., et al. (2008). Attribution of polar warming to human influence. *Nature Geoscience*, *1*(11), 750–754. https://doi.org/10.1038/ngeo338

Graham, R. M., Hudson, S. R., & Maturilli, M. (2019). Improved performance of ERA5 in Arctic gateway relative to four global atmospheric reanalyses. *Geophysical Research Letters*, *46*(11), 6138–6147. https://doi.org/10.1029/2019GL082781

Graversen, R. G., Mauritsen, T., Tjernstrom, M., Kallen, E., & Svensson, G. (2008). Vertical structure of recent Arctic warming. *Nature*, *451*(7174), 53–56. https://doi.org/10.1038/nature06502

Guttu, S., Orsolini, Y., Stordal, F., Otteraa, O. H., & Omrani, N. (2021). The 11-year solar cycle UV irradiance effect and its dependency on the Pacific Decadal Oscillation. *Environmental Research Letters*, *16*(6), 64030. https://doi.org/10.1088/1748-9326/abfe8b

Hahn, L. C., Armour, K. C., Zelinka, M. D., Bitz, C. M., & Donohoe, A. (2021). Contributions to polar amplification in CMIP5 and CMIP6 models. *Frontiers of Earth Science*, *9*, 710036. https://doi.org/10.3389/feart.2021.710036

He, S., Xu, X., Furevik, T., & Gao, Y. (2020). Eurasian cooling linked to the vertical distribution of Arctic warming. *Geophysical Research Letters*, *47*(10), e2020G–e87212G. https://doi.org/10.1029/2020GL087212

Henderson, G. R., Barrett, B. S., Wachowicz, L. J., Mattingly, K. S., Preece, J. R., & Mote, T. L. (2021). Local and remote atmospheric circulation drivers of Arctic change: A review. *Frontiers of Earth Science*, *9*, 549. https://doi.org/10.3389/feart.2021.709896

Hersbach, H., Bell, B., Berrisford, P., Biavati, G., Horányi, A., Muñoz Sabater, J., et al. (2019). ERA5 monthly averaged data on pressure levels from 1979 to present [Dataset]. Copernicus Climate Change Service (C3S) Climate Data Store (CDS). https://doi.org/10.24381/cds.6860a573

Hersbach, H., Bell, B., Berrisford, P., Hirahara, S., Horányi, A., Muñoz-Sabater, J., et al. (2020). The ERA5 global reanalysis. *Quarterly Journal of the Royal Meteorological Society*, *146*(730), 1999–2049. https://doi.org/10.1002/qj.3803

Hirdman, D., Burkhart, J. F., Sodemann, H., Eckhardt, S., Jefferson, A., Quinn, P. K., et al. (2010). Long-term trends of black carbon and sulphate aerosol in the Arctic: Changes in atmospheric transport and source region emissions. *Atmospheric Chemistry and Physics*, *10*(19), 9351–9368. https://doi.org/10.5194/acp-10-9351-2010

Hourdin, F., Rio, C., Grandpeix, J., Madeleine, J., Cheruy, F., Rochetin, N., et al. (2020). LMDZ6A: The atmospheric component of the IPSL climate model with improved and better tuned physics. *Journal of Advances in Modeling Earth Systems*, *12*(7), e1892M–e2019M. https://doi.org/10.1029/2019MS001892

Kaufmann, R. K., Kauppi, H., Mann, M. L., & Stock, J. H. (2011). Reconciling anthropogenic climate change with observed temperature 1998–2008. *Proceedings of the National Academy of Sciences*, *108*(29), 11790–11793. https://doi.org/10.1073/pnas.1102467108

Keenlyside, N. S., Latif, M., Jungclaus, J., Kornblueh, L., & Roeckner, E. (2008). Advancing decadal-scale climate prediction in the North Atlantic sector. *Nature*, *453*(7191), 84–88. https://doi.org/10.1038/nature06921

Labe, Z., Peings, Y., & Magnusdottir, G. (2018). Contributions of ice thickness to the atmospheric response from projected Arctic sea ice loss. *Geophysical Research Letters*, *45*(11), 5635–5642. https://doi.org/10.1029/2018GL078158

Labe, Z., Peings, Y., & Magnusdottir, G. (2020). Warm Arctic, cold Siberia pattern: Role of full Arctic amplification versus sea ice loss alone. *Geophysical Research Letters*, *47*(17), e2020G–e88583G. https://doi.org/10.1029/2020GL088583

Landrum, L. L., & Holland, M. M. (2022). Influences of changing sea ice and snow thicknesses on simulated Arctic winter heat fluxes. *The Cryosphere*, *16*(4), 1483–1495. https://doi.org/10.5194/tc-16-1483-2022

Lang, A., Yang, S., & Kaas, E. (2017). Sea ice thickness and recent Arctic warming. *Geophysical Research Letters*, *44*(1), 409–418. https://doi.org/10.1002/2016GL071274

Li, F., Orsolini, Y. J., Wang, H., Gao, Y., & He, S. (2018). Atlantic multidecadal oscillation modulates the impacts of Arctic sea ice decline. *Geophysical Research Letters*, *45*(5), 2497–2506. https://doi.org/10.1002/2017GL076210

Liang, Y., Frankignoul, C., Kwon, Y., Gastineau, G., Manzini, E., Danabasoglu, G., et al. (2021). Impacts of Arctic sea ice on cold season atmospheric variability and trends estimated from observations and a multi-model large ensemble. *Journal of Climate*, *34*(20), 8419–8443. https://doi.org/10.1175/JCLI-D-20-0578.1

Liang, Y., Polvani, L. M., & Mitevski, I. (2022). Arctic amplification, and its seasonal migration, over a wide range of abrupt CO_2 forcing. *Npj Climate and Atmospheric Science*, *5*(1), 14. https://doi.org/10.1038/s41612-022-00228-8

Mantua, N. J., & Hare, S. R. (2002). The Pacific decadal oscillation. *Journal of Oceanography*, *58*(1), 35–44. https://doi.org/10.1023/A:1015820616384

Matthes, K., Funke, B., Andersson, M. E., Barnard, L., Beer, J., Charbonneau, P., et al. (2017). Solar forcing for CMIP6 (v3.2). *Geoscientific Model Development*, *10*(6), 2247–2302. https://doi.org/10.5194/gmd-10-2247-2017

Meehl, G. A., Hu, A., Arblaster, J. M., Fasullo, J., & Trenberth, K. E. (2013). Externally forced and internally generated decadal climate variability associated with the interdecadal Pacific oscillation. *Journal of Climate*, *26*(18), 7298–7310. https://doi.org/10.1175/JCLI-D-12-00548.1

Met Office Hadley Centre. (2016). Hadley Centre sea ice and sea surface temperature data set [Dataset]. HadISST.2. Retrieved from https://www.metoffice.gov.uk/hadobs/hadisst2/

Mochizuki, T., Ishii, M., Kimoto, M., Chikamoto, Y., Watanabe, M., Nozawa, T., et al. (2010). Pacific decadal oscillation hindcasts relevant to near-term climate prediction. *Proceedings of the National Academy of Sciences*, *107*(5), 1833–1837. https://doi.org/10.1073/pnas.0906531107

Omrani, N. E., Keenlyside, N. S., Bader, J., & Manzini, E. (2014). Stratosphere key for wintertime atmospheric response to warm Atlantic decadal conditions. *Climate Dynamics*, *42*(3), 649–663. https://doi.org/10.1007/s00382-013-1860-3

Parker, D. E., Wilson, H., Jones, P. D., Christy, J. R., & Folland, C. K. (1996). The impact of Mount Pinatubo on world-wide temperatures. *International Journal of Climatology*, *16*(5), 487–497. https://doi.org/10.1002/(SICI)1097-0088(199605)16:5<487::AID-JOC39>3.0.CO;2-J

Perlwitz, J., Hoerling, M., & Dole, R. (2015). Arctic tropospheric warming: Causes and linkages to lower latitudes. *Journal of Climate*, *28*(6), 2154–2167. https://doi.org/10.1175/JCLI-D-14-00095.1

Polvani, L. M., & Waugh, D. W. (2004). Upward wave activity flux as a precursor to extreme stratospheric events and subsequent anomalous surface weather regimes. *Journal of Climate*, *17*(18), 3548–3554. https://doi.org/10.1175/1520-0442(2004)017<3548:UWAFAA>2.0.CO;2

Ren, L., Yang, Y., Wang, H., Zhang, R., Wang, P., & Liao, H. (2020). Source attribution of Arctic black carbon and sulfate aerosols and associated Arctic surface warming during 1980–2018. *Atmospheric Chemistry and Physics*, *20*(14), 9067–9085. https://doi.org/10.5194/acp-20-9067-2020

Robock, A. (2000). Volcanic eruptions and climate. *Reviews of Geophysics*, *38*(2), 191–219. https://doi.org/10.1029/1998RG000054

Santer, B. D., Wigley, T. M. L., Boyle, J. S., Gaffen, D. J., Hnilo, J. J., Nychka, D., et al. (2000). Statistical significance of trends and trend differences in layer-average atmospheric temperature time series. *Journal of Geophysical Research*, *105*(D6), 7337–7356. https://doi.org/10.1029/1999JD901105

Screen, J. A., & Deser, C. (2019). Pacific Ocean variability influences the time of emergence of a seasonally ice-free Arctic ocean. *Geophysical Research Letters*, *46*(4), 2222–2231. https://doi.org/10.1029/2018GL081393

Screen, J. A., Deser, C., & Simmonds, I. (2012). Local and remote controls on observed Arctic warming. *Geophysical Research Letters*, *39*(10), L10709. https://doi.org/10.1029/2012GL051598

Screen, J. A., & Simmonds, I. (2010a). The central role of diminishing sea ice in recent Arctic temperature amplification. *Nature*, *464*(7293), 1334–1337. https://doi.org/10.1038/nature09051

Screen, J. A., & Simmonds, I. (2010b). Increasing fall-winter energy loss from the Arctic Ocean and its role in Arctic temperature amplification. *Geophysical Research Letters*, *37*(16), L16707. https://doi.org/10.1029/2010GL044136

Seland, Ø., Bentsen, M., Olivié, D., Toniazzo, T., Gjermundsen, A., Graff, L. S., et al. (2020). Overview of the Norwegian Earth System Model (NorESM2) and key climate response of CMIP6 DECK, historical, and scenario simulations. *Geoscientific Model Development*, *13*(12), 6165–6200. https://doi.org/10.5194/gmd-13-6165-2020

Stenchikov, G., Robock, A., Ramaswamy, V., Schwarzkopf, M. D., Hamilton, K., & Ramachandran, S. (2002). Arctic Oscillation response to the 1991 Mount Pinatubo eruption: Effects of volcanic aerosols and ozone depletion. *Journal of Geophysical Research*, *107*(D24), 21–28. https://doi.org/10.1029/2002JD002090

Stevens, B., Giorgetta, M., Esch, M., Mauritsen, T., Crueger, T., Rast, S., et al. (2013). Atmospheric component of the MPI-M Earth system model: ECHAM6. *Journal of Advances in Modeling Earth Systems*, *5*(2), 146–172. https://doi.org/10.1002/jame.20015

Sun, H., Zhou, G., & Zeng, Q. (2012). Assessments of the climate system model (CAS-ESM-C) using IAP AGCM4 as its atmospheric component. *Chinese Journal of Atmospheric Sciences*, *36*(2), 215. https://doi.org/10.3878/j.issn.1006-9895.2011.11062

Sun, L., Allured, D., Hoerling, M., Smith, L., Perlwitz, J., Murray, D., & Eischeid, J. (2018). Drivers of 2016 record Arctic warmth assessed using climate simulations subjected to Factual and Counterfactual forcing. *Weather and Climate Extremes*, *19*, 1–9. https://doi.org/10.1016/j.wace.2017.11.001

Suo, L., Gao, Y., Gastineau, G., Liang, Y., Ghosh, R., Tian, T., et al. (2022). Datasets for publication "Arctic troposphere warming driven by external radiative forcing and modulated by the pacific and Atlantic" [Dataset]. Norwegian research infrastructure services (NRIS). http://ns9015k.web.sigma2.no/BlueAct/

Svendsen, L., Keenlyside, N., Bethke, I., Gao, Y., & Omrani, N. (2018). Pacific contribution to the early twentieth-century warming in the Arctic. *Nature Climate Change*, *8*(9), 793–797. https://doi.org/10.1038/s41558-018-0247-1

Ting, M., Kushnir, Y., Seager, R., & Li, C. (2009). Forced and internal twentieth-century SST trends in the North Atlantic. *Journal of Climate*, *22*(6), 1469–1481. https://doi.org/10.1175/2008JCLI2561.1

Titchner, H. A., & Rayner, N. A. (2014). The met Office Hadley Centre sea ice and sea surface temperature data set, version 2: 1. Sea ice concentrations. *Journal of Geophysical Research: Atmospheres*, *119*(6), 2864–2889. https://doi.org/10.1002/2013JD020316

Tokinaga, H., Xie, S., & Mukougawa, H. (2017). Early 20th-century Arctic warming intensified by Pacific and Atlantic multidecadal variability. *Proceedings of the National Academy of Sciences*, *114*(24), 6227–6232. https://doi.org/10.1073/pnas.1615880114

Trenberth, K. E., & Hurrell, J. W. (1994). Decadal atmosphere-ocean variations in the Pacific. *Climate Dynamics*, *9*(6), 303–319. https://doi.org/10.1007/BF00204745

Woo, S., Sung, M., Son, S., & Kug, J. (2015). Connection between weak stratospheric vortex events and the Pacific Decadal Oscillation. *Climate Dynamics*, *45*(11), 3481–3492. https://doi.org/10.1007/s00382-015-2551-z

Yang, F., & Schlesinger, M. E. (2002). On the surface and atmospheric temperature changes following the 1991 Pinatubo volcanic eruption: A GCM study. *Journal of Geophysical Research*, *107*(D8), 1–8. https://doi.org/10.1029/2001JD000373

Yu, Y., Xiao, W., Zhang, Z., Cheng, X., Hui, F., & Zhao, J. (2021). Evaluation of 2-m air temperature and surface temperature from ERA5 and ERA-I using buoy observations in the Arctic during 2010–2020. *Remote Sensing*, *13*(14), 2813. https://doi.org/10.3390/rs13142813

Zhang, R., Wang, H., Fu, Q., Pendergrass, A. G., Wang, M., Yang, Y., et al. (2018). Local radiative feedbacks over the Arctic based on observed short-term climate variations. *Geophysical Research Letters*, *45*(11), 5761–5770. https://doi.org/10.1029/2018GL077852

Zhang, R., Wang, H., Fu, Q., Rasch, P. J., Wu, M., & Maslowski, W. (2021). Understanding the cold season Arctic surface warming trend in recent decades. *Geophysical Research Letters*, *48*(19), e2021G–e94878G. https://doi.org/10.1029/2021GL094878

Zhang, Y., Wallace, J. M., & Battisti, D. S. (1997). ENSO-like interdecadal variability: 1900–93. *Journal of Climate*, *10*(5), 1004–1020. https://doi.org/10.1175/1520-0442(1997)010<1004:ELIV>2.0.CO;2